Line-shape analyses of XVV Auger spectra of $p(1\times1)$-$V_3Si(100)$: Evidence for autoionization emission

G. Zajac, J. Zak,* and S. D. Bader
Materials Science and Technology Division, Argonne National Laboratory, Argonne, Illinois 60439
(Received 17 February 1983)

In the light of recent advances in understanding the Auger process, the local electronic structural origins of selected core-valence-valence (XVV) Auger line shapes are analyzed for a transition-metal silicide prototype, V_3Si. We report for clean $p(1\times1)$-$V_3Si(100)$ Auger spectra that include the region of the vanadium $M_{2,3}VV$ and M_1VV and the Si $L_{2,3}VV$ transitions. We compare the measured line shapes to spectra we generated based on the muffin-tin local density of states (DOS) calculated self-consistently by Klein *et al.* Good agreement in both the Si $pp(L_{2,3}M_{2,3}M_{2,3})$ and the V $dd(M_{2,3}M_{4,5}M_{4,5})$ peak positions between experiment and calculation verified that the final-state hole-hole repulsion for Si (U_{pp}) and V (U_{dd}) are both ~0 eV. Also, the Si $L_{2,3}VV$ spectrum resembles that of elemental Si in that the line shape is predominantly a self-fold of the Si $3p$ DOS. However, an unexpected result is that the V spectral region above the $M_{2,3}VV$ threshold possesses a broad (~30-eV-wide) intense feature that is not amenable to conventional interpretation in terms of the M_1VV transition or $M_{2,3}VV$ double-ionization or plasmon-gain satellites. We attribute this observation to the presence of Fano autoionization emission associated with deexcitation of the resonant $3p\rightarrow3d$ transition. Supporting evidence comes from a comparison of our x-ray- and electron-stimulated Auger spectra, and to the line shape of the $3p$ loss spectrum. In addition, oxygen-dosing Auger and x-ray photoelectron spectroscopy experiments (0—20 L) (1 langmuir = 1 L = 10^{-6} Torr sec) indicate dramatic Si $L_{2,3}VV$ line-shape changes associated with oxidation, similar to that observed previously for Pd_4Si. The initial oxidation rate is $\sim10^2$ faster than that for elemental Si. We hypothesize that the dissociation of O_2 is a rate-determining step in the oxidation of elemental Si, but is rapid at transition-metal sites in the silicides. Atomic oxygen then rapidly spills over to the neighboring silicon sites where oxidation subsequently occurs.

I. INTRODUCTION

The recent progress in understanding the local electronic structural information contained in core-valence-valence (XVV) Auger transitions of both silicon[1,2] and the transition metals[3,4] enables one to attempt fundamental Auger studies of more complex systems. We have chosen V_3Si as a prototype for such a study due to the availability of high-quality single crystals and state-of-the-art band-structure calculations.[5–7] Intense theoretical[8] and experimental[9] interest in V_3Si stems from its very interesting superconductive and related normal-state properties, which are governed by electronic states near the Fermi energy E_F. Comparisons of band calculations to experiments that probe not only the region near E_F, but the entire band structure, have also been made, i.e., x-ray photoelectron spectroscopy[10] (XPS), soft x-ray emission spectroscopy,[11] and angle-resolved ultraviolet photoelectron spectroscopy (ARUPS).[12] The present comparison to Auger electron spectroscopy falls in this latter category. In particular, the region of the MVV Auger transitions of vanadium and the $L_{2,3}VV$ of silicon are examined and compared to self-folds of local densities of states (DOS) obtained from the band-structure calculations of Klein *et al.*[5] Final-state hole-hole repulsion energies for the silicon p band (U_{pp}) and vanadium d band (U_{dd}) are extracted and found to be ~0 eV. The spectral region of vanadium above the $M_{2,3}VV$ threshold presents the greatest challenge, in that it is not amenable to a simple band-structure interpretation, but indicates the existence of many-body effects associated with electron-stimulated Fano autoionization emission associated with coupling to vanadium $3p$ core-level excitations. We also find that the initial oxidation properties radically differ from those of elemental silicon.[13,14] Oxygen dosing (0—20 L) (1 L = 1 langmuir = 10^{-6} Torr sec) of the $p(1\times1)-V_3Si(100)$ indicates rapid oxidation of the

silicon sites, which is consistent with an earlier study[15,16] of another transition-metal (TM) silicide Pd_4Si. Dissociative adsorption of O_2 at the TM site, followed by rapid spillover and oxidation of the Si site, is postulated.

The outline of the remainder of the paper is as follows. Section II contains experimental and calculational details, including cleaning procedures, and a description of a $p(2\times1)$ reconstruction observed in the course of the study. In Sec. III the Auger spectra of the V $M_{2,3}VV$, M_1VV, and Si $L_{2,3}VV$ regions are presented with the results for the removal of losses. Calculated self-folds for the three Auger transitions are introduced and compared to experiment. A variety of possible many-body influences are evaluated for the challenging M_1VV-$M_{2,3}VV$ gain region. Oxygen-dosing results are then presented and discussed. Finally, the main results are summarized in Sec. IV.

II. METHODS

A. Experimental procedures

The experiments were performed in a bakeable stainless-steel UHV system (base pressure 2×10^{-10} Torr) equipped with 4-grid low-energy electron diffraction (LEED) optics, residual gas analyzer, x-ray source, and double-pass cylindrical-mirror analyzer (CMA) with coaxial electron gun, as described previously.[15,16] Undifferentiated Auger spectra for the line-shape analyses were taken typically with a 2-keV primary energy, $\sim$10-μA beam current, and no modulation voltage applied to the outer cylinder, but half-cycle blanking of the electron-gun emission and "analog pulse counting" using a lock-in amplifier. The amplifier output was digitized and stored on disk for subsequent analysis. Electron-energy-loss spectroscopy (EELS) data taken for background correction of the Auger spectra utilized 90-, 230-, and 500-eV primary-beam energies. XPS measurements were taken with a Mg$K\alpha$ source to obtain core-level binding energies for the Si and V $2p$ levels. The V_3Si single crystal ($5\times4\times1$ mm^3) was mounted to a tantalum heater backing by Ta straps which could be resistively heated to 1500 °C. A Chromel-Alumel thermocouple was placed under one of the Ta straps in close thermal contact with the crystal. The sample temperature was additionally measured by an optical pyrometer, viewed through a quartz window at normal incidence.

B. Sample and surface preparations

The V_3Si(100) crystal was prepared by Dr. A. J. Arko of the Argonne National Laboratory. A floating-zone method was used, and the crystal was mechanically polished and etched in aqua regia. Similar such crystals have been used in de Haas–van Alphen and ARUPS studies.[12]

The optimal cleaning procedure was carefully studied to eliminate trace-oxygen contamination, which is not readily detected by Auger analysis due to overlap of the KVV transition at 506 eV (^{506}O) with the ^{503}V L_3VV transition. Such trace oxygen could obscure the Si $L_{2,3}VV$ line-shape analysis, due to formation of Si oxide.[17] First, repeated Ar^+-ion sputtering at 500 eV followed by prolonged annealing ($\lesssim$8 h) at 750 °C was used. This cleaning pro-

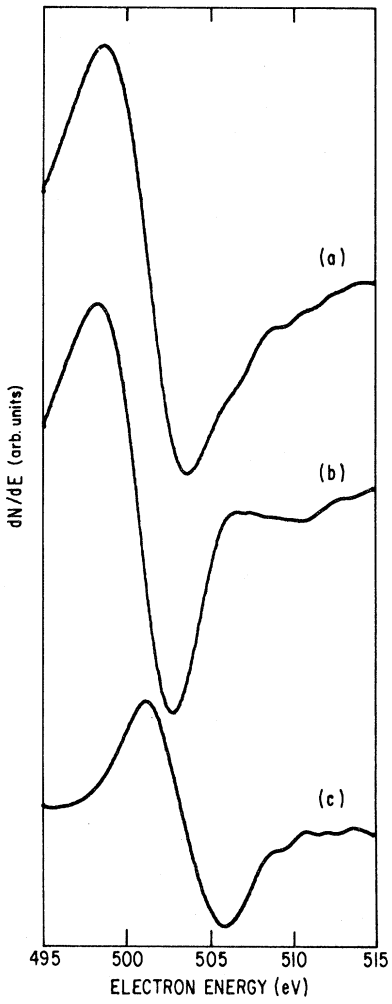

FIG. 1. Auger derivative spectra taken at 0.5-eV peak-peak modulation, for two different cleaning procedures: (a) 500-eV ion bombardment and 750 °C anneal; note asymmetry of V L_3VV signal due to oxygen KVV interference. (b) Same region scanned after 1300 °C in 1×10^{-6} Torr hydrogen with 750 °C anneal. (c) Difference plot of curves (a) and (b) showing a small residual oxygen signal present after "standard" cleaning procedure.

cedure ensured a sharp $p(1\times1)$ LEED pattern with no detectable $p(2\times1)$ reconstruction spots, as will be discussed in Sec. II C. The major impurities were removed by this cleaning method, although trace amounts of oxygen were believed present. High-resolution differentiated Auger spectra (0.5-eV peak-to-peak modulation) of this "clean" V_3Si revealed a high-energy shoulder which was assumed to be submonolayer oxygen contamination. [See Fig. 1(a).] To remove this trace-oxygen impurity a new cleaning procedure was adopted. The sample was flashed to 1300 °C in 1×10^{-6} Torr hydrogen for 5 min, then annealed for several hours at 750 °C to produce a sharp $p(1\times1)$ LEED pattern. The results of this cleaning procedure are detailed in Fig. 1(b). Panel (c) of Fig. 1 is the (a)-(b) difference plot, which reveals that a small residual oxygen signal [$\sim$0.06 monolayer (ML)] was present before hydrogen flashing. This latter cleaning procedure resulted in a clean V_3Si surface free of oxygen to within 0.01 ML.

The oxygen dosing was begun after a clean surface was obtained as described above. The O_2 pressure for dosing was 1×10^{-7} Torr. After each dose the electron beam was turned "on" and an Auger, XPS, or EELS scan was recorded. An interesting effect was found in the XPS study of the V 2*p* core level. Rapid V oxidation occurred when the oxygen dosing was performed with the electron beam turned "on" but was not observed with it "off". The inference is that electron-beam-induced oxidation of the V sites was occurring. This effect was not observed in the case of the oxidation of the Si sites, the electron beam always being "off" during the O_2-dosing period.

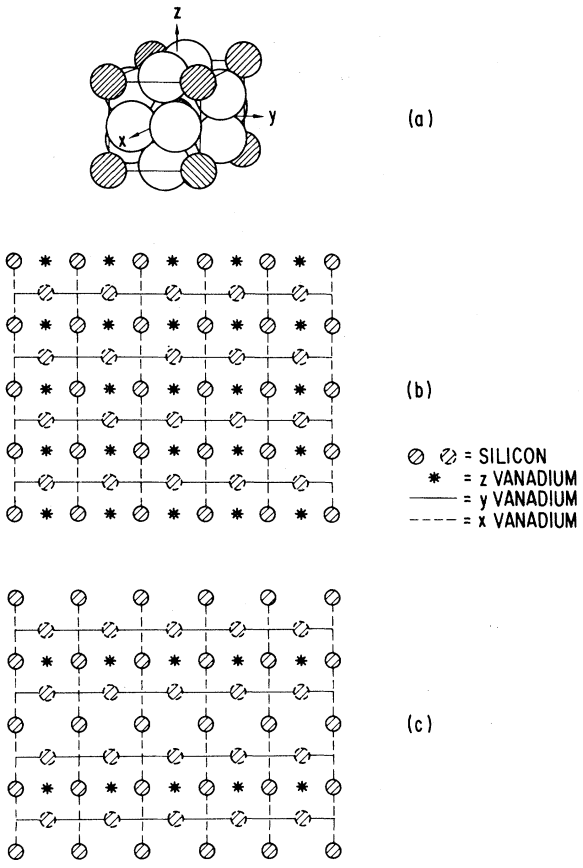

FIG. 2. $p(2\times1)$ reconstruction model for $V_3Si(100)$. (a) V_3Si unit cell; solid circles are silicon and open circles are vanadium atoms. (b) Representation of unreconstructed (100) face. (c) Representation of $p(2\times1)$ reconstruction model; note depletion of surface vanadium atoms.

C. Characterization of the $p(2\times1)$ LEED reconstruction

Heating of the clean $p(1\times1)$-$V_3Si(100)$ crystal to temperatures in excess of 800 °C resulted in reconstruction with a single-domain $p(2\times1)$ LEED pattern. The ratio of vanadium (31 eV) to silicon (92 eV) peak-to-peak heights would decrease 8.6% from 0.95 for the $p(1\times1)$ to 0.87 for the $p(2\times1)$, suggestive of vanadium depletion driving the reconstruction. Since the *A*-15 unit cell[8,9] of V_3Si consists of silicons at bcc locations and linear chains of two vanadiums on each face in all three perpendicular directions [Fig. 2(a)], it is possible to develop a simple reconstruction model for the $p(2\times1)$ and calculate the Auger vanadium-to-silicon ratio for comparison to experiment. Since the *x* and *y* vanadium chains lie in the surface plane they should be present equally on the surface, due to the existence of steps. Hence any reconstruction involving these chains would not tend to give rise to a single-domain $p(2\times1)$ pattern, as observed, but would consist of a $p(2\times1)+p(1\times2)$ superposition. Thus presumably the V chains perpendicular to the surface are involved. A simple one-layer reconstruction model for the $p(2\times1)$-$V_3Si(100)$ would involve missing V atoms at the termination of alternating *z*-axis chains, as shown in Fig. 2.

To test this model we calculated the ^{31}V-to-^{92}Si Auger ratio and compared it to experiment. Consider that the ratio (ξ_E) of intensity of Auger electrons at a given energy (E) from an alloy to that from the pure metal is given by[18]

$$\xi_E=\frac{\sum_{n=1}^{\infty}\chi_n^i\exp(-z_n^{\text{alloy}}/\lambda_E\cos\theta)}{f\sum_{n=1}^{\infty}\exp(-z_n^i/\lambda_E\cos\theta)}, \tag{1}$$

where $f=(a^{\text{alloy}}/a)^2$, χ_n^i is the concentration of the ith component in-layer n, λ_E is the escape depth of an electron at energy E, θ is the angle of collection (43° for CMA), and z_n represents the perpendicular distance from the surface of layer n. With the use of the lattice constants $a^{\text{alloy}}=4.722$ Å, $a^{\text{V}}=3.0399$ Å, and $a^{\text{Si}}=5.53035$ Å, and escape depths for the vanadium of 8.0 Å and silicon of 5.5 Å, the sums in Eq. (1) are calculated (terminating after four lattice constants into the bulk because of the small escape depths involved). The measured quantities are the normalized peak ratios

$$\frac{R(E/E')}{R^0(E/E')}=\frac{I_E}{I_{E'}}\left[\frac{I_E^0}{I_{E'}^0}\right]^{-1}=\frac{\xi_E}{\xi_{E'}}\,, \tag{2}$$

where E and E' refer to the ^{31}V and ^{92}Si Auger transitions, respectively. The resultant ratio change for the proposed $p(1\times1)$-to-$p(2\times1)$ reconstruction model is 8.8%, in close agreement with the experimental value of 8.6%. This supports the simple one-layer reconstruction model of Fig. 2(b), which involves vacancies on alternating rows of the topmost z-chain V sites. It would be quite interesting to see how well this model would stand up to more direct surface-structural studies of $p(2\times1)$-$V_3Si(100)$.

D. Method of Auger self-fold calculation

The Auger self-fold calculation was performed utilizing the angular momentum decomposed local DOS for V_3Si from Klein *et al.*[5] A transition density function N' is generated as follows:

$$N'(E)=N_L(E)+\alpha_{L'}N_{L'}(E)\,, \tag{3}$$

where $\alpha_{L'}$ weighs the L' band relative to the L band ($L,L'=s$, p, or d), where V s,p,d and Si s,p contributions are retained, and $LL'=ss$, pp, dd, sp, or pd. The $N'(E)$ was first Gaussian broadened (0.7 eV) to simulate realistic cumulative analyzer resolution, core-hole lifetime, and spin-orbit splitting effects, as was done previously.[19] Finally the Auger self-fold is[20]

$$A(2E)\propto\int_0 N'(E+\epsilon)N'(E-\epsilon)d\epsilon\,, \tag{4}$$

where the limits of integration are from the Fermi energy $E_F=0$ to E, if $0<E<E_B/2$, and 0 to E_B-E, if $E_B/2<E<E_B$, where E_B is the binding energy of the bottom of the occupied valence band.

E. Loss-correction method

Although loss-correction procedures are well documented,[21–23] we present our analysis here for the

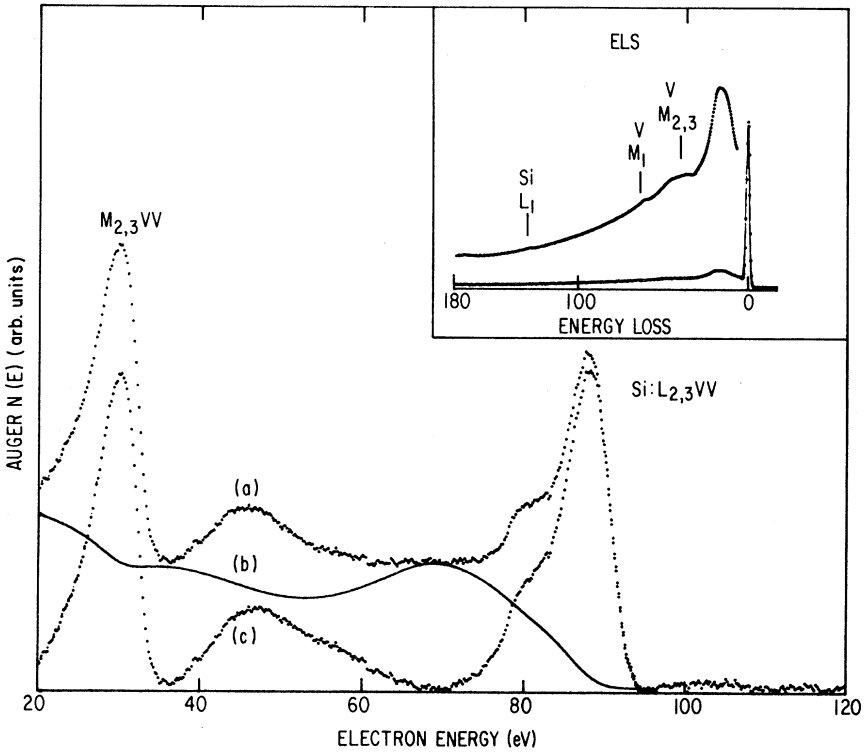

FIG. 3. Auger spectrum of clean $p(1\times1)$-$V_3Si(100)$. (a) Raw data uncorrected for losses. (b) Loss background [(a)-(c)] generated using EELS data shown in inset. (c) Loss-corrected Auger spectra showing V MVV and Si $L_{2,3}VV$ regions.

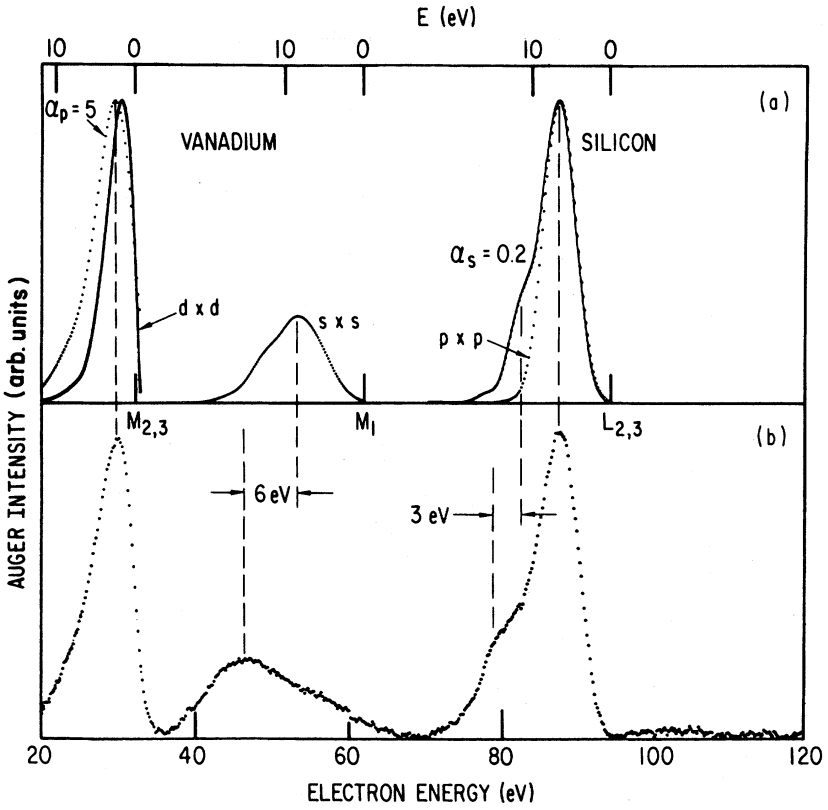

FIG. 4. Calculated Auger self-folds comparison to loss-corrected experimental data of Fig. 3. (a) Self-folds of the local densities of states for V_3Si. On the left, the $M_{2,3}VV$ of vanadium dominated by *dd* self-fold (dotted curve). In the middle, the M_1VV of vanadium given by the pure *ss* self-fold. On the right, the $L_{2,3}VV$ of silicon given by the pure *pp* (dotted curve) and 20% *s* character included (solid curve). (b) The experimental line shapes taken from Fig. 3.

record, since we have not done so before. For each energy E, starting from the largest value, a corrected spectral intensity I_c for all $E' < E$ is found from the expression

$$I_c(E') = I(E') - (1-f)I(E)L(E-E') , \quad (5)$$

where I is initially the measured spectrum, L is the loss function, where the zero-loss energy is positioned at E, and f is an empirical constant, independent of E, to take into account that loss generation is not identical in EELS and Auger processes, due, for instance, to intrinsic losses, etc. The I and L spectra are, in general, corrected for the analyzer-transmission function before generating I_c. The loss function is normalized to unit area under the elastic peak, and then the elastic peak is removed to yield L. This procedure is quite similar to that of Madden and Houston[22] except that we do not deconvolute out the width of the elastic peak from the Auger spectrum. Note that our procedure is fast in that no iterations are necessary, as is required by the van Cittert's technique used in Ref. 22.

III. RESULTS

A. Loss correction of *XVV* Auger spectra of V_3Si

Figure 3(a) shows a raw Auger spectrum that includes the V $M_{2,3}VV$, M_1VV, and Si $L_{2,3}VV$ regions from left to right. The inset shows the electron-loss spectrum used to subtract the losses. The loss background stripped from the Auger spectrum of curve (a) is shown in curve (b), and the loss-corrected Auger spectrum appears in curve (c). Notice that the loss removal has not shifted peak positions but has reduced the low-energy shoulder of the Si $L_{2,3}VV$ (75—85 eV) and has modified the high-energy side of the 50—70-eV region.

B. The V $M_{2,3}VV$ transition

Results of Auger self-fold calculations for the transitions of interest are shown in Fig. 4(a), along with the experimental results from Fig. 3(c) reproduced below them. Core-level threshold energies are

indicated based on XPS binding energies shifted by ϕ_a, our analyzer work function, so that we can retain the experimental electron-energy scale. Comparison of the experimental and calculated V $M_{2,3}VV$ transitions, shown at the left of Fig. 4, indicates that a pure *dd* self-fold (dotted calculation) provides the dominant contribution to the line shape. This is in good agreement with the results for copper where the $M_{2,3}VV$ line is *d*-like according to the calculated Auger matrix elements.[24] In copper the *dd* Auger decay for the $M_{2,3}$ level is of much higher probability than the *ds* and *ss* decays. One expects a similar situation to exist in vanadium and the agreement of the theoretical *dd* fold with experimental $M_{2,3}$ line shape is indeed very good (see Fig. 4). Note that calculated heights are normalized approximately to the experimental ones in Fig. 4. The agreement in peak positions between the $M_{2,3}VV$ experiment and calculation implies that the hole-hole repulsion U_{dd} is ~ 0 eV. This is in agreement with previously published results.[25] The asymmetry that appears on the low-energy side of the $M_{2,3}VV$ experimental spectrum can be accounted for by inclusion of some *pd* character to the transition, as is shown in Fig. 4. The α_p value of 5 seems large, but the *d*-character weighting within the muffin-tin spheres about the V sites is so much greater than either *s* or *p* character, that the *pd* term is still just a shoulder superimposed on the dominant *dd* term in Fig. 4. Alternately, the experimental low-energy asymmetry may be due, in part, to electron-hole pair production,[21,26] as would be expected for a high DOS material, and is evident in the Doniach-Sunjic asymmetry[27] of the core-level XPS peaks. Finally, shortcomings of the loss-correction procedure for such low kinetic energy electrons, due to the true secondary electrons, will influence this spectral region.

C. The Si $L_{2,3}VV$ transition

The Si $L_{2,3}VV$ transition (to the right in Fig. 4) is seen to be dominated by a *pp* self-fold, as in elemental Si.[2] By contrast, in Pd_4Si, where the Si 3*s* band is localized,[15] it was found that there is considerable *s* participation in this transition ($\alpha_s^{Pd_4Si} \sim 1$). In V_3Si the Si 3*s* band is unhybridized and split off below the V-derived bands[5]; hence, by analogy to Pd_4Si a considerable *s* contribution was expected. This transition appears intermediate between those observed for elemental Si ($\alpha_s^{Si} \sim 0$) and Pd_4Si in that there *is* a significant, though small ($\alpha_s^{V_3Si} \sim 0.2$), *sp* low-energy shoulder, as is shown in Fig. 4. The origin of the 3-eV positional discrepancy between experiment and the calculated *sp* shoulder in Fig. 4 is not well un-

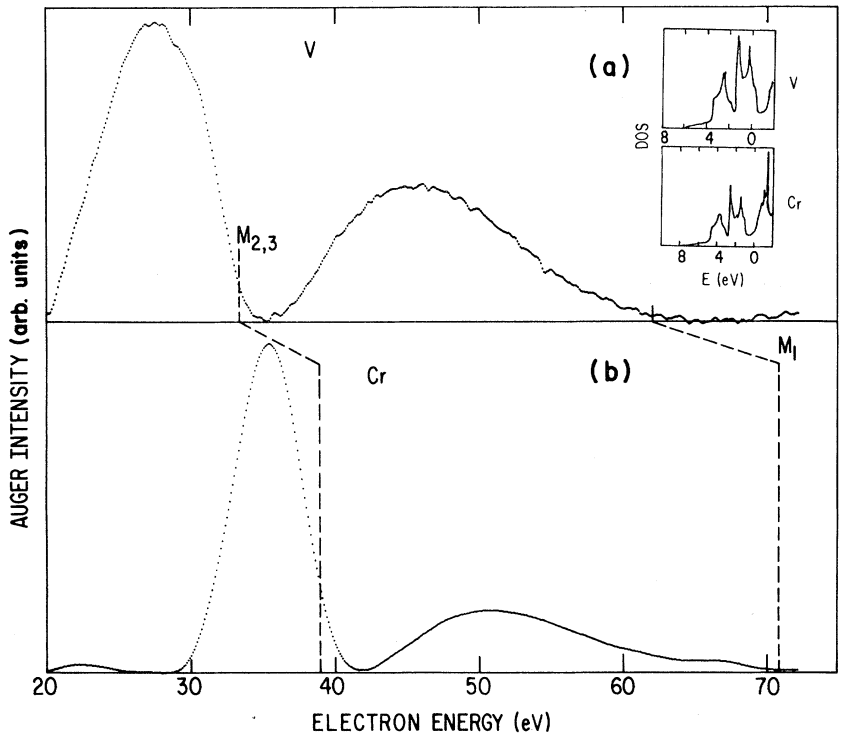

FIG. 5. Experimental *MVV* Auger transitions for elemental (a) vanadium and (b) chromium; inset shows calculated valence bands from Ref. 32. The M_1 and $M_{2,3}$ thresholds are indicated.

derstood, but may, at least in part, be due to an underestimate of the Si 3*s* binding energy in the Klein *et al.* calculation[5] (~1 eV), as has been suggested previously based on a photoemission comparison[12] to the calculated DOS. Finally, the agreement in peak positions between experiment and calculation implies a value of $U_{pp} \sim 0$ eV, as was the case for elemental Si (Refs. 1 and 2) and Pd_4Si (Ref. 15).

D. The *V* spectral region between 35–65 eV

The *MVV* region of V (Fig. 4, center) is the source of the greatest challenge to our understanding of the Auger process. We present our evaluation of numerous effects indicating, as we shall see, the breakdown of single-particle theory by many-body effects.

1. *Unsuccessful attempts at an M_1VV analysis*

The single asymmetric feature of Fig. 4 has an unusually broad basewidth of ~30 eV, and terminates near the M_1 threshold. Thus we start by attempting to treat this feature as an M_1VV transition. The best attempt to fit the line shape to single-particle theory then involves a self-fold of the V *s* DOS, as shown in Fig. 4. However, the experimental peak is 6 eV lower in energy than the calculated *ss* peak. We found that the use of the Cini theory[28] to calculate the renormalization of the single-particle result due to a two-hole final-state repulsive interaction U_{ss} of 6 eV brings the calculated line shape into quantitative agreement with experiment. However, this is misleading since a 6-eV U_{ss} is unjustifiable. The atomic U_{ss} is 6.8 eV for bare holes, based on Mann's calculations[29]; if one includes intra-atomic relaxation and solid-state screening effects one would expect a much smaller value of U_{ss}. It *is* plausible that $U_{ss} > 0$, since the *d* screening electrons of V may be ineffective in fully screening *s* holes from each other, much in the same manner that the *s* screening electrons of Cu do not fully screen the *d* holes from each other. (In Cu the bare atomic value of U_{dd} is ~28 eV, while the solid-state value is ~8 eV).[30] However, U_{ss} should be much smaller than 6 eV and cannot explain the 6-eV shift between the experimental and theoretical curves in the 35–65-eV region of Fig. 4. Thus we eliminate the two-hole interaction as being central to understanding this spectral region.

Also, we note that the *ss* assumption is severe in that some *d* involvement is expected. It has been shown that *dd* and *sd* terms dominate the M_1VV transitions of Cu (Ref. 4) and Ni (Ref. 31). Also, for these latter elements the M_1VV spectral intensity is minor ($\sim 10^{-1}$) compared to that of the $M_{2,3}VV$ transition. The reason that a self-fold of the V *s* DOS yielded the experimental basewidth can be found in the Klein *et al.* calculations.[5] The Si 3*s* contribution at 7.7-eV binding energy is radially extended, spills over into the V muffin-tin spheres, and adds spectral weight to the bottom of V *s* DOS. For elemental V the *s* DOS is narrower[32]; thus if this spectral region is due to an *ss* dominated M_1VV transition, it should be correspondingly *sharper* in V than in V_3Si. Figure 5 shows the elemental V Auger spectrum we measured to check this point. (There is an arbitrary spline background[23] removed from the data, and the inset shows the V DOS calculated by Moruzzi *et al.*[32]) Note that the experimental spectral region is much greater than twice the calculated M_1VV bandwidth. Similar information is displayed also for elemental Cr in Fig. 5. Thus we conclude that the broad basewidth we report is a general property, at least in this part of the Periodic Table, and that an *ss*-dominated M_1VV transition is not the cause.

2. *Unsuccessful attempts at $M_{2,3}VV$ hypersatellite analyses*

Another possible explanation of the unusual broad feature of the transition in question is to assume that it may be dominated by a high-energy $M_{2,3}VV$

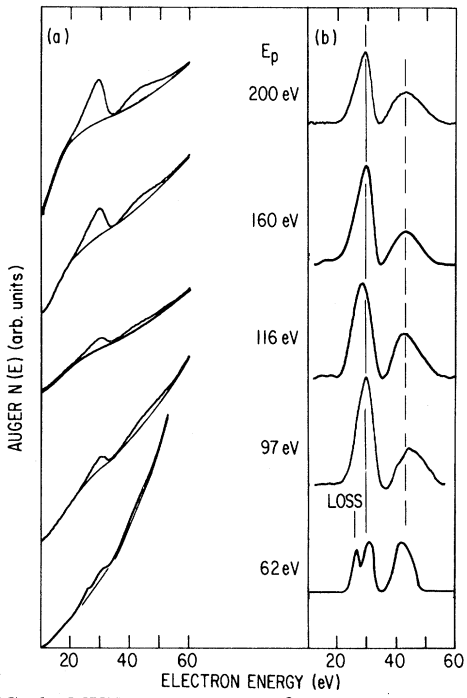

FIG. 6. *MVV* Auger spectra of elemental vanadium for indicated primary energies. (a) Raw spectra; (b) enlargements with arbitrary splined background [shown in (a)] removed. The vertical bar labeled "loss" for the 62-eV primary beam is the $M_{2,3}$ core loss feature.

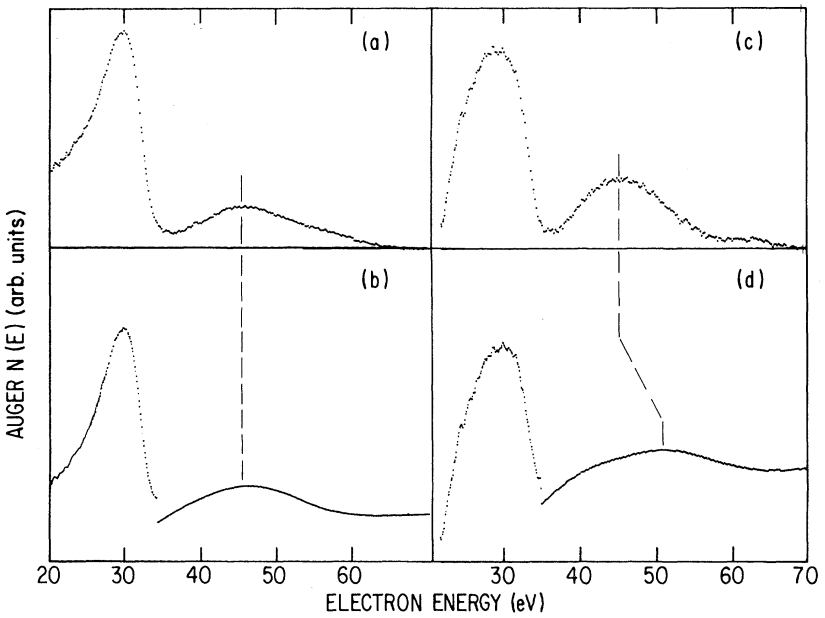

FIG. 7. Plasmon-gain satellites. (a) Experimental spectra; (b) calculated gain satellite by utilizing EELS spectra of Fig. 12 for $M_{2,3}VV$ of $V_3Si(100)$; (c) 20-L O_2 experimental spectra; (d) calculated gain satellite of 20-L O_2 spectra.

satellite. Two types of such hypersatellites have been discussed in the literature: (a) a doubly ionized initial state,[33,34] and (b) a plasmon-gain satellite.[35,36] We rule out an $M_{2,3}M_{2,3}$ doubly ionized initial-state basis for the postulated $M_{2,3}VV$ satellite because the direct production cross section for this initial state is small, and an Auger production due to L or $M_1M_{2,3}M_{2,3}$ transitions would predict that the satellite would vanish when the primary-beam energy E_p drops below the intial-state ionization threshold E_L or E_{M_1}. We see in Fig. 6 that the satellite in the elemental vanadium spectrum is still prominent for $E_p < E_{M_1} \ll E_L$. Furthermore, energetically we expect this satellite to appear at <6 eV energy gain, based on the difference in $E_{M_{2,3}}$ of V and Cr.[33]

We now consider a plasmon-gain mechanism as a basis for an $M_{2,3}VV$ satellite in the M_1VV spectral region. To test the plasmon-gain hypothesis we generated such a satellite from the $M_{2,3}VV$ and EELS data by inverting the loss-subtraction procedure outlined in Sec. II E. The calculated and measured gain satellites appear in Figs. 7(a) and 7(b), respectively. The agreement in peak position and width is quite good. [Note that the discontinuity in Fig. 7(b) occurs where the data were set to zero, before convoluting in the gain features.] To further extend the methodology, as shown in Figs. 7(c) and 7(d), we applied this model to an oxidized surface, whose characterization is given in Sec. III E. [Note that the Auger data in Figs. 7(a) and 7(c) are loss and analyzer transmission function corrected spectra from Fig. 10. The EELS data used appears in Fig. 12.] The agreement between experiment and calculation here is unsatisfactory (even though possible interference from cross transitions[37] due to maximal valency of V complicates the situation). Thus we give additional consideration to plasmon coupling before ruling it out.

A plasmon-gain mechanism implies a rapid Auger process[35,36,38] otherwise plasmons would propagate or decay away from the site of interest before coupling to the Auger electron could take place. The MVV transitions are expected to be rapid, since super Coster-Kronig (MMM) channels are involved. Kowalczyk[39] measured the widths (inverse lifetimes) of the elemental V M_1 and $M_{2,3}$ XPS core levels and found 2.6 and 1.2 eV full width at half maximum (FWHM), respectively, after removal of analyzer broadening. The relatively narrow $M_{2,3}$ width seems to preclude the dynamical criterion. It is of interest to note that Watts[36] has discussed the possibility of differentiating between two types of plasmon-gain couplings. The conventional dynamical process[36,38] considered above involves coupling to a plasmon created by the initial core hole, while the energetic primary particle independently creates a plasmon sea and core holes in the second (Jenkins-Chung[35]) process. Since x-rays are ineffective in directly exciting a plasmon sea, Watts[36] suggested that this latter process would be discriminated against in x-ray versus electron-stimulated Auger

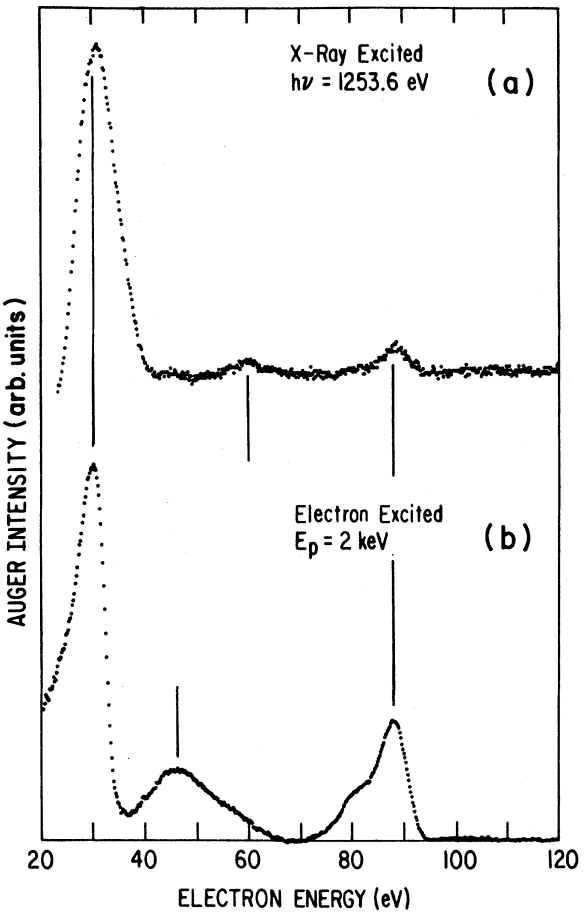

FIG. 8. X-ray (Mg K_α) excited (a) vs electron (2 keV), (b) Auger spectra of $V_3Si(100)$. The e^- excited spectrum is that of Fig. 4 corrected for the analyzer transmission function, while the x-ray excited spectrum also has a smooth spline background function removed.

experiments, although to our knowledge this has never been followed up. Figure 8 shows the first such comparison, where there is a striking difference between the spectra. The x-ray-excited Auger spectrum contains only the expected $M_{2,3}VV$ and M_1VV transitions and not the anomalously broad feature observed so clearly upon electron excitation. However, in the Sec. III D 3 we will present a more plausible and convincing explanation of the dramatic difference.

3. *Autoionization emission explanation*

Thus far we have established that there is a broad ($\sim$30 eV wide) and intense high-energy satellite above the vanadium $M_{2,3}VV$ Auger transition of $V_3Si(100)$. This feature is general in nature in that it is also present in elemental vanadium and, with somewhat reduced intensity, in Cr, as is shown in Fig. 5. There is also a degree of chemical sensitivity in that the satellite is somewhat enhanced upon oxidation (see Fig. 7). Most importantly, the satellite is electron but not x-ray stimulated (see Fig. 8). We have explored the applicability of conventional interpretations, which involve the M_1VV Auger transition and $M_{2,3}VV$ double-ionization and plasmon-gain origins. We conclude that none of these possibilities provide satisfactory explanations of our observations.

We propose that this $M_{2,3}VV$ gain satellite is due to Fano autoionization emission.[40,41] This process involves the following: First, an $M_{2,3}$ ($3p$) core hole is created by promotion of a $3p$ electron to an unfilled $M_{4,5}$ level (denoted d^*) above the Fermi level (not by removing the $3p$ electron from the solid, as occurs upon x-ray irradiation). Subsequently, the $3p$ hole decays by being filled with the d^* electron and

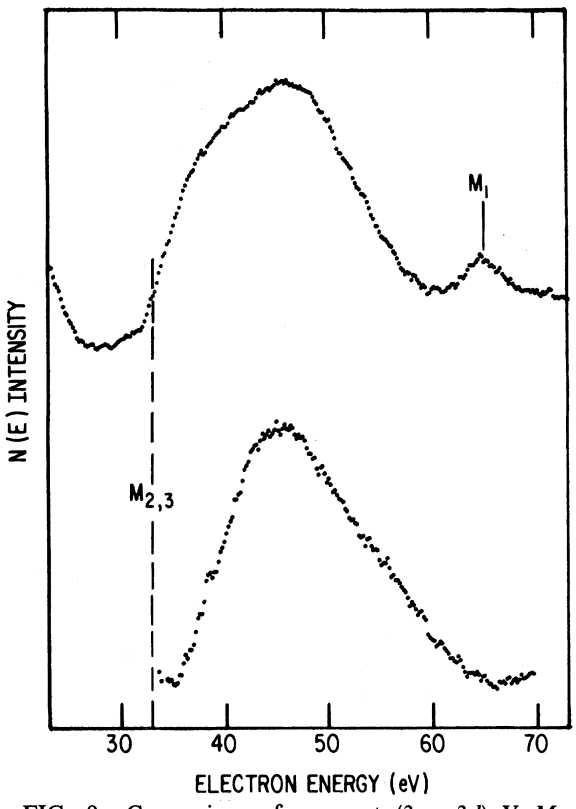

FIG. 9. Comparison of resonant ($3p \rightarrow 3d$) V $M_{2,3}$ EELS absorption spectrum of V_3Si ($E_p = 232$ eV) (upper curve) to the autoionization emission spectrum (lower curve) (taken from central region of Fig. 4). The EELS line is shifted with respect to the emission spectra 4 eV to smaller energies to account for the analyzer work function. The M_1 absorption threshold is also indicated in the EELS spectrum.

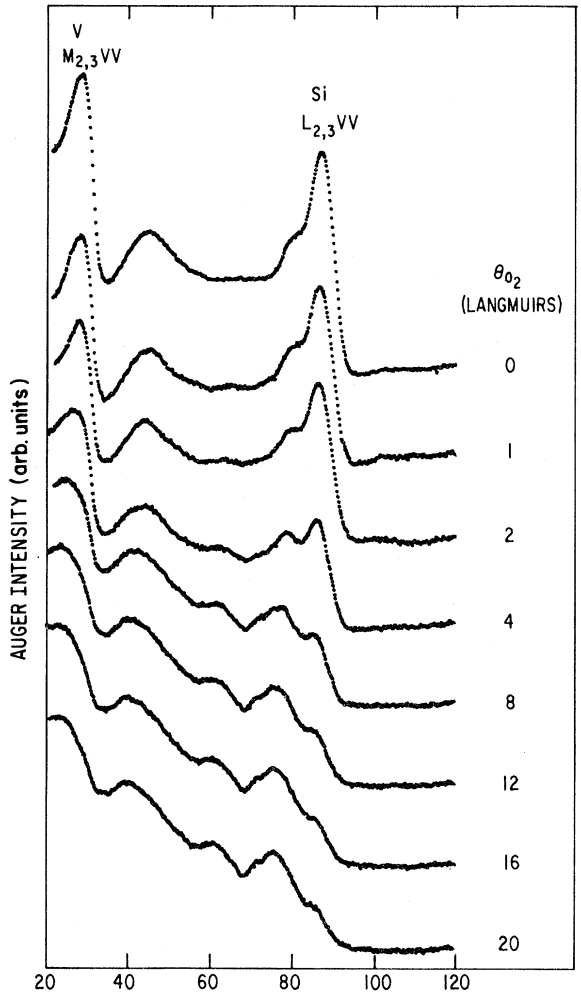

FIG. 10. Oxygen-dosing V_3Si Auger results. Note SiO_2-like peaks at 60 and 75 eV after 20-L exposure.

emitting a d electron (or vice versa) to conserve energy. The width of the feature in question is due to the interference of $p \rightarrow d^*$ with energetically equivalent $d \rightarrow \epsilon f$ channels, where ϵf denotes continuum f states that are projected out of the plane-wave-like states well above E_F. Configuration interaction between $p \rightarrow d^*$ and $d \rightarrow \epsilon f$ channels causes the d^* states above E_F to lose the narrow, quasi-discrete character they possess in the ground state (absence of $3p$ hole) and take on broad continuum character of autoionization levels.[42,43] The process can be summarized as

$$3p^6d^n \underset{(1)}{\rightarrow} 3p^5d^nd^* \underset{(2)}{\rightarrow} 3p^6d^{n-1}+\epsilon f \ , \qquad (6)$$

where the first step involves *absorption* of energy from the primary electron beam, and the second step involves autoionization *emission* of the ϵf electron.

To test this proposal we expect the (ϵf emission) feature we observe above the $M_{2,3}VV$ Auger threshold to be similar in intensity and line shape to that of the $M_{2,3}$ core-level loss spectrum. Comparison of the two processes is shown in Fig. 9, where the primary-beam energy was reduced to 232 eV in order to conveniently collect absorption and emission spectra in a single 200-eV scan. The emission threshold has been corrected for the analyzer work function, i.e., $E_{\text{threshold}}=E_{\text{core}}-\phi_a(4.0\text{ eV})$. Note that both spectra peak at ~ 13 eV above the $M_{2,3}$ threshold. Rigorous identity between the two spectra is not expected since finite collection angles are necessarily employed, approximate (proportional to E) transmission function corrections are used, etc.[41] Comparisons that are similarly gratifying for elemental V, Cr, Ni, and Cu have been obtained and will be reported elsewhere.[44] It is of value to note that intensity trends with position in the Periodic Table, and upon oxidation, mentioned at the beginning of this section, can be readily understood within the present framework, since it is well known from the classic work of Robins and Swan[45] that the intensity and the width of the $M_{2,3}$ loss spectrum (near-edge structure) increase with the number of d holes. Therefore, the autoionization emission should be more intense in the beginning of the $3d$ transition-metal series than at the end where there are fewer d holes. Correspondingly, it should also be more intense for oxidized V compared to clean V, as is observed (Fig. 10).

E. Oxygen-dosing effects

Oxygen dosing the clean $p(1\times 1)$-$V_3Si(100)$ leads to dramatic line-shape changes in the $L_{2,3}VV$ of silicon and the $M_{2,3}VV$ of vanadium (Fig. 10). The clean (0-L dose) spectrum (Fig. 10) is the equivalent of the spectrum used for the Auger analysis (Fig. 3). The Si $L_{2,3}VV$ transition undergoes major redistribution by 4 L, which is drastically different from the case of elemental Si where doses are 10^2 times larger for equivalent changes in line shape.[46] Comparison to published Auger spectra of the Si $L_{2,3}VV$ in SiO_2 (Ref. 17) allows identification of spectral features attributable to SiO_2 at 60 and 75 eV, while the shoulder at 85 eV corresponds to a small residual unoxidized subsurface silicon signal. Since the escape depth at 85–90 eV is ~ 5 Å, this indicates there exists ~ 1–2 ML of SiO_2-like species on the surface after a 20-L O_2 exposure. Additionally, the $M_{2,3}VV$ transition shifts to lower energy and considerably broadens. All major changes occur by 8–12-L exposures.

To further elucidate the rapid oxidation of the Si sites, XPS was used to monitor the $2p$ core levels of

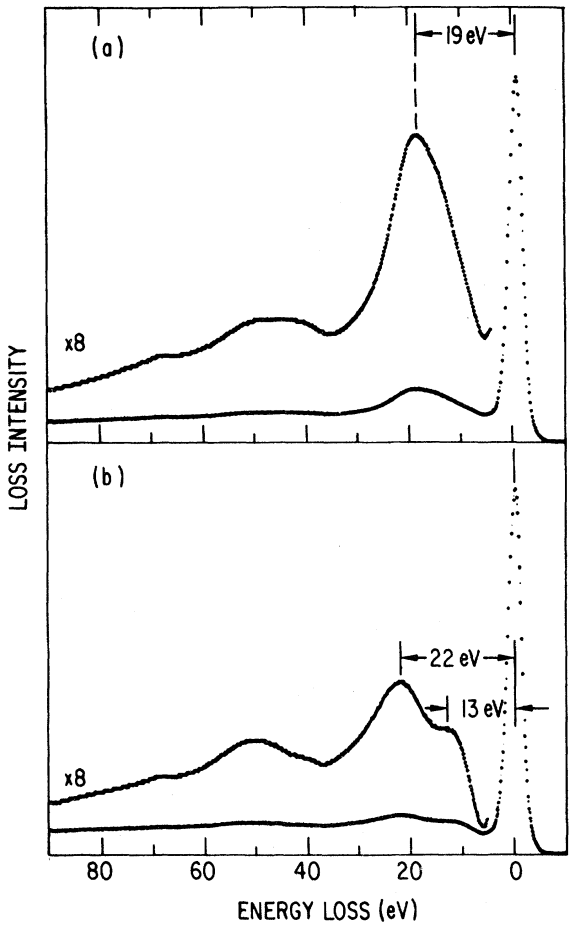

FIG. 12. Electron-energy-loss spectra for (a) clean V_3Si and (b) 20-L O_2, taken at a primary-beam energy of 500 eV.

both the Si and V (Fig. 11). The binding energy of the Si $2p$ emission of clean V_3Si is found to be 98.5 ± 0.2 eV, in excellent agreement with that reported in Ref. 7. The high binding-energy peak at 103.0 eV that develops by 20-L O_2 exposure corresponds to a SiO_2-like species, based on the 4.5-eV chemical shift. (In elemental Si the $2p$ binding energy is 99.2 eV, and it shifts 4.2—103.4 eV in SiO_2.[14]) Similarly the V $2p_{3/2}$ binding energy in V_3Si is 511.2 ± 0.2 eV (elemental V $2p_{3/2}$ is 511.95 eV (Refs. 12 and 47) and also shows rapid oxidation by 20 L, at which point further Si oxidation may be diffusion limited and, thus, V is attacked. (As was pointed out in Sec. II B, the V sites could be oxidized more readily if an electron beam were left on during the O_2 dosing.) Note also in Fig. 11 that the clean V $2p$ emission is highly asymmetric in the Doniach-Sunjic sense, as is expected due to electron-hole-pair production in a high-DOS material. Finally, the oxygen $1s$ emission overlaps with the V $2p$ loss satellite, in Fig. 11; thus XPS is not as sensitive a probe of O contamination as the Auger analysis presented in Sec. II B and Fig. 1. Loss spectra for the O_2-dosed surface are shown in Fig. 12.

The rapid Si oxidation is believed to be due to dissociation of the O_2 molecule at the vanadium sites, followed by spillover to the Si sites, where rapid oxidation occurs. The implication is that the rate-determining step in the oxidation of elemental Si is O_2 dissociation. Here it is of interest to note that Garner *et al.*[14] reported that steps or hot filaments accelerate the oxidation of elemental Si. Hot filaments presumably excite the O_2 molecule to a metastable state that facilitates subsequent dissociative adsorption, while steps might provide active sites for dissociation. Indeed, rapid oxidation of elemental Si, due to atomic O-beam impingement on the surface, was observed long ago.[48] Rossi *et al.*[49] have recently reported enhanced Si-oxidation rates due to submonolayer Ag coating of Si surfaces prior to O_2 dosing. This is presumably identical to the effect reported herein, and previously for the initial Si oxidation of Pd_4Si.[15,16] V, Ag, and Pd, and all transition metals readily dissociatively chemisorb the O_2 molecule at room temperature.

IV. SUMMARY OF CONCLUSIONS

The line shapes of Auger transitions of V_3Si in the Si $L_{2,3}VV$, and V $M_{2,3}VV$, and M_1VV regions were analyzed utilizing angular momentum decomposed local DOS calculations of Klein *et al.*[5] The Si $L_{2,3}VV$ and V $M_{2,3}VV$ transitions were dominated by *pp* and *dd* contributions, respectively, with hole-hole repulsion energies ~0 eV in both cases. This indicates that these two-hole Auger final states are fully screened, as expected. Low-energy shoulders associated with each of these transitions may contain *sp* and *pd* character, respectively. It is usually believed that for *s-p* band materials, such as Si, the core-valence-valence Auger line shapes can be understood in terms of unperturbed valence-band densities of states. On the other hand, *d*-band metals have Auger line shapes that do not resemble the valence-band density of states. V_3Si is an example of a material where the band structure is given by both *s-p* and *d* orbitals. Our results show that the Auger line shapes of this material are quite well described by the valence-band density of states, the Si $L_{2,3}VV$ line by the *pp* fold (as in elemental Si), and the V $M_{2,3}VV$ line by the *dd* fold. The case for the V spectral region above the $M_{2,3}VV$ threshold presented a totally different problem, in that even qualitative description of the main characteristics (peak width, position, and intensity) is a challenge.

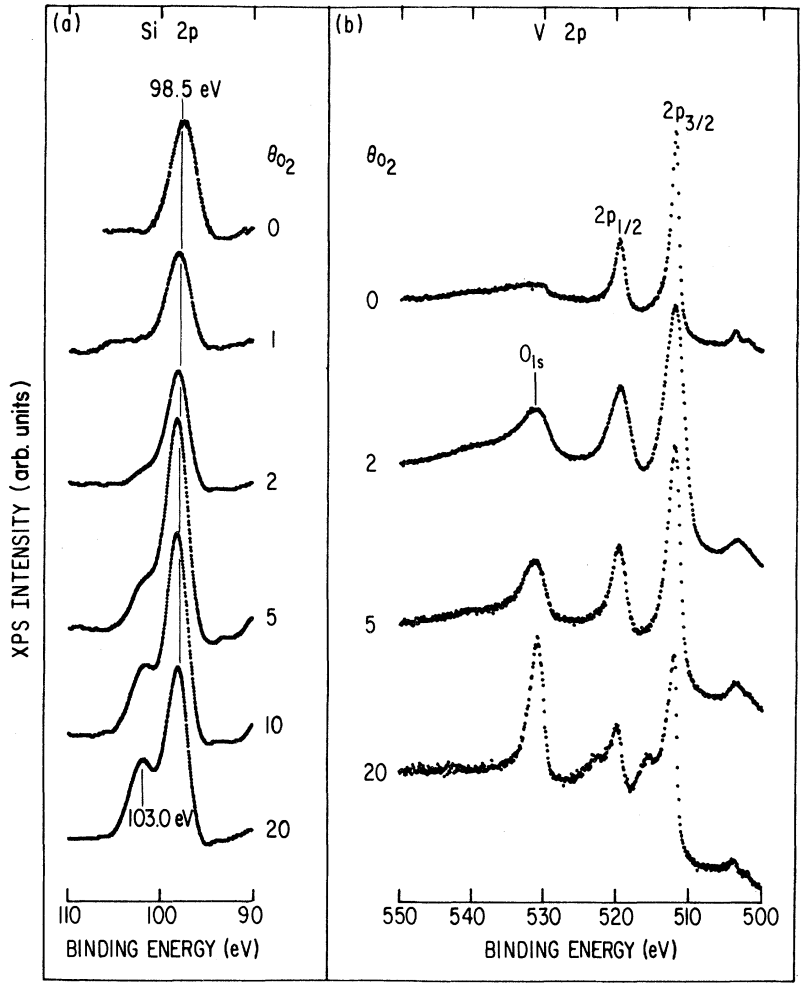

FIG. 11. XPS oxygen-dosing V_3Si results. (a) Si $2p$ and (b) V $2p$. Note oxygen appears in the loss region of the V $2p$ emission. The vanadium $2p_{3/2}$ binding energy is 511.2 ± 0.2 eV.

We conclude that this spectral region is not amenable to band-structure interpretation, but that it contains an autoionization emission associated with coupling to $3p$ core-level excitations of vanadium. This finding should stimulate renewed interest in the *MVV* spectra of all the $3d$ transition metals.

Finally, oxygen-dosing experiments of V_3Si show dramatic Si initial oxidation rates relative to those for elemental Si.[46] It is believed that O_2 dissociatively chemisorbs readily on all transition-metal silicide TM sites at room temperature, and that then rapid O spillover to Si sites occurs, where oxidative attack ensues. Comparison to previous studies, especially for palladium silicide,[15,16] supports these ideas.

While we have observed that great progress can be made in understanding the electronic structural origin of even the most challenging Auger features for the complex prototype we have chosen to investigate, further work, both experimental and theoretical in nature, would be welcomed.

ACKNOWLEDGMENTS

We thank A. J. Arko for generously providing the V_3Si single-crystal, O. Bisi, T. Jarlborg, and B. M. Klein for providing detailed tables of the V_3Si density-of-states decomposition, and R. J. Friddle for technical support.

*Permanent address: Department of Physics, Technion—Israel Institute of Technology, Haifa 32000, Israel.

[1]P. J. Feibelman, E. J. McGuire, and K. C. Pandey, Phys. Rev. Lett. 36, 1154 (1976); Phys. Rev. B 15, 2202 (1977); P. J. Feibelman and E. J. McGuire, *ibid.* 17, 690 (1978).

[2]D. R. Jennison, Phys. Rev. Lett. 40, 807 (1978); Phys. Rev. B 18, 6865 (1978).

[3]G. A. Sawatzky and A. Lenselink, Phys. Rev. B 21, 1790 (1980), and references therein.

[4]D. R. Jennison, Phys. Rev. B 18, 6996 (1978).

[5]B. M. Klein, L. L. Boyer, D. A. Papaconstantopoulos, and L. F. Mattheiss, Phys. Rev. B 18, 6411 (1978).

[6]G. Arbman and T. Jarlborg, Solid State Commun. 26, 857 (1978); T. Jarlborg, J. Phys. F 9, 283 (1979).

[7]O. Bisi and L. W. Chiao, Phys. Rev. B 25, 4943 (1982).

[8]M. Weger and I. B. Goldberg, in *Solid State Physics,* edited by H. Ehrenreich, F. Seitz, and D. Turnbull (Academic, New York, 1973), Vol. 28.

[9]L. R. Testardi, in *Physical Acoustics,* edited by W. P. Mason and R. N. Thurston (Academic, New York, 1973), Vol. X, p. 193.

[10]J. Riley, J. Azoulay, and L. Ley, Solid State Commun. 19, 993 (1976); P. O. Nilsson, I. Curelaru, and T. Jarlborg, Phys. Status Solidi B 79, 277 (1977).

[11]E. Z. Kurmaev, V. P. Belash, S. A. Nemnonov, and A. S. Shulakov, Phys. Status Solidi 61, 365 (1974).

[12]M. Aono, F. J. Himpsel, and D. E. Eastman, Solid State Commun. 39, 225 (1981).

[13]H. Ibach, K. Horn, R. Dorn, and H. Lüth, Surf. Sci. 38, 433 (1973).

[14]C. M. Garner, I. Lindau, C. Y. Su, P. Pianetta, and W. E. Spicer, Phys. Rev. B 19, 3944 (1979).

[15]S. D. Bader, L. Richter, M. B. Brodsky, W. E. Brower, and G. V. Smith, Solid State Commun. 37, 729 (1981).

[16]S. D. Bader, L. Richter, and T. W. Orent, Surf. Sci. 115, 501 (1982).

[17]D. E. Ramaker, J. S. Murday, N. H. Turner, G. Moore, M. G. Lagally, and J. Houston, Phys. Rev. B 19, 5375 (1979); D. E. Ramaker, *ibid.* 21, 4608 (1980).

[18]J. M. McDavid and S. C. Fain, Surf. Sci. 52, 161 (1975).

[19]G. Zajac and S. D. Bader, Phys. Rev. B 26, 5688 (1982).

[20]G. F. Amelio and E. J. Scheibner, Surf. Sci. 11, 242 (1968); C. J. Powell, Phys. Rev. Lett. 30, 1179 (1973).

[21]R. Weissman and K. Müller, Surf. Sci. Rep. 105, 251 (1981).

[22]H. H. Madden and J. E. Houston, J. Appl. Phys. 47, 3071 (1976).

[23]P. Staib and J. Kirschner, Appl. Phys. 3, 421 (1974).

[24]E. J. McGuire, Phys. Rev. A 16, 2365 (1977).

[25]Lo I. Yin and Tung Tsang, Phys. Rev. B 15, 2974 (1977).

[26]P. H. Citrin, G. K. Wertheim, and Y. Baer, Phys. Rev. B 16, 4256 (1977).

[27]S. Doniach and M. Sunjić, J. Phys. C 3, 285 (1970).

[28]M. Cini, Solid State Commun. 20, 605 (1976); 24, 681 (1977); Phys. Rev. B 17, 2788 (1978).

[29]J. B. Mann, Los Alamos Scientific Laboratory Report No. LASL-3690 (unpublished).

[30]E. Antonides and G. A. Sawatzky, in *Proceedings of the International Conference on the Physics of Transition Metals, Toronto 1977,* edited by M. J. G. Lee, J. M. Perz, and E. Fawcett (IOP, London, 1978), p. 134.

[31]S. D. Bader (unpublished).

[32]V. L. Moruzzi, J. F. Janak, and A. R. Williams, *Calculated Electronic Properties of Metals* (Pergamon, New York, 1978), p. 73.

[33]W. F. Hamson and E. T. Arakawa, Z. Phys. 251, 271 (1972).

[34]E. J. McGuire, in *Atomic and Inner-Shell Processes,* edited by B. Crasemann (Academic, New York, 1975), Vol. I, p. 293.

[35]L. H. Jenkins and M. F. Chung, Surf. Sci. 26, 151 (1971).

[36]C. M. K. Watts, J. Phys. F 2, 574 (1972).

[37]Y. Fukuda and A. Ignatiev, Solid State Commun. 41, 597 (1982).

[38]O. Gunnarsson and K. Schönhammer, Phys. Rev. B 22, 3710 (1980).

[39]S. Kowalczyk, Ph.D. thesis, University of California, Berkeley, 1976 (unpublished).

[40]U. Fano, Phys. Rev. 124, 1866 (1961).

[41]V. V. Balashov, S. S. Lipovetskii, and V. S. Senashenko, Zh. Eksp. Teor. Fiz. 63, 1622 (1972) [Sov. Phys.—JETP 36, 858 (1972)].

[42]R. E. Dietz, E. G. McRae, Y. Yafet, and C. W. Caldwell, Phys. Rev. Lett. 33, 1372 (1974).

[43]L. C. Davis and L. A. Feldkamp, Phys. Rev. B 23, 6239 (1981).

[44]S. D. Bader, G. Zajac, and J. Zak, Phys. Rev. Lett. 50, 1211 (1983).

[45]J. L. Robins and J. B. Swan, Proc. Phys. Soc., London 76, 857 (1960).

[46]S. Tougaard, P. Morgan, and J. Onsgaard, Surf. Sci. 111, 545 (1981).

[47]D. A. Shirley, R. L. Martin, S. P. Kowalczyk, F. R. McFeeley, and L. Ley, Phys. Rev. B 15, 544 (1977); in *Photoemission in Solids I,* Vol. 26 of *Topics in Applied Physics,* edited by M. Cardona and L. Ley (Springer, Berlin, 1978), p. 265.

[48]R. J. Madix and A. A. Susu, Surf. Sci. 20, 377 (1970).

[49]G. Rossi, L. Caliari, I. Abbati, L. Braicovich, I. Lindau, and W. E. Spicer, Surf. Sci. Lett. 116, L202 (1982).